Rev. Roum. Sci. Techn.– Électrotechn. et Énerg.
Vol. **68**, *1*, pp. 52–57, Bucarest, 2023

COMPARISON OF THE VARIOUS CONTROLS OF THE SWITCHED RELUCTANCE MOTOR 12/8

MAMA CHOUITEK[1], ABDELLAH CHAOUCH[2], BENAISSA BEKKOUCHE [2]

Keywords: Switched reluctance machine (SRM); Proportional–integral–derivative (PID) controller; Neural command; Fuzzy logic control.

The control of the variable reluctance machine raises a certain number of constraints, among which we can cite: the effect of the external disturbances, the nature of the nonlinearities, the ripple of its torque, and the modeling errors. The different ordering approaches proposed in this article dealt with all these constraints. The classical-control algorithms, for example, of derived full proportional action may prove sufficient if the requirements on the accuracy and performance of systems are flexible. In the opposite case, particularly when the controlled part is submitted to strong nonlinearity and temporal variations, control techniques must be designed to ensure the process's robustness concerning the uncertainties on the parameters and their variations. These techniques include artificial intelligence-based techniques constituted of neural networks and fuzzy logic. This technique can replace PID regulators with nonlinear ones using the human brain's reasoning and functioning and is simulated using MATLAB/Simulink software. Finally, by using obtained waveforms, these results will be compared.

1. INTRODUCTION

The SRM (switched reluctance machine) is a double salience machine, *i.e.*, with stator and rotor poles, and this structure produces a high output torque. Although the structure of SRM is doubly protruding, there are no winding or permanent magnets in the rotor, which simplifies the machine's structure and contributes to the low manufacturing cost.

However, despite these positive attributes, switched reluctance drive exhibits higher acoustic noise and vibration [1,2]. However, its inductance varies with temperature and level of magnetic saturation; the evolution of this parameter during the machine's operation affects the machine's dynamic performance and its average torque, which strongly depends on it and deteriorates. There is also the presence of noise due to the static converter.

It is, therefore, necessary to design high-performance controls that are less sensitive to these parametric variations and these disturbances. A current line of research is based on artificial intelligence tools such as fuzzy logic and neural network.

2. EQUIVALENT CIRCUIT AND ELECTROMAGNETIC EQUATIONS

The SRM 12/8 has 12 stator poles and 8 rotor poles. The phases of the stator are A, B and C. Each phase consists of 4 stator poles (A_1,A_2,A_3,A_4; B_1,B_2,B_3,B_4; C_1,C_2,C_3,C_4).The poles of a same phase are shifted by $\pi/2$ radians shown in Fig.1) [3-4]. Phases A, B and C are offset by $\pi/6$ radians from each other. The parameters used for the 12/8 motor in Fig. 1 are shown in Table 1.

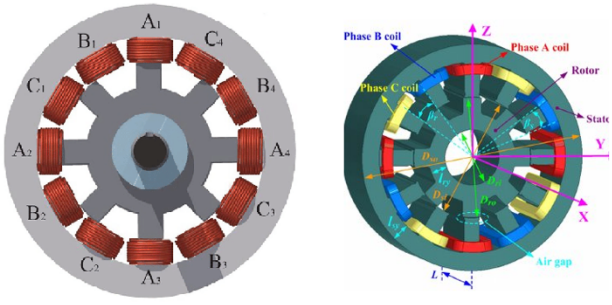

Fig. 1 – The switched reluctance motor.

The equivalent circuit of a phase of the *SRM* is composed of a resistance R_s, an inductance $L(\theta)$, and an *emf* *e*, connected in series, as shown in Fig 2.

Table 1

Parameters used for the 12/8 motor

Phases number	N_p	3
Number of stator poles	N_s	12
Number of rotor poles	N_r	8
Nominal power	P_n [KW]	3
Nominal voltage	V_n[V]	380
Nominal current	I_n[A]	13
Speed of motor	ω [rd/s]	200
Electromagnetic torque	T [N.m]	12
Stator resistor	R_s [Ω]	1.3
Maximal inductance	L_{max} [mH]	90
Minimum inductance	L_{min} [mH]	60
Magnetic Induction	B [T]	0,0183
Moment of inertia	J [Kg.m^2]	0.0013
Stator pole arc	β_s [°]	15
Rotor pole arc	β_r [°]	16

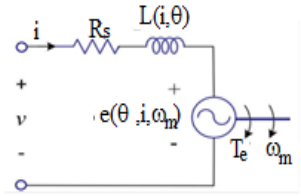

Fig. 2 – Equivalent circuit of an SRM phase

Neglecting the mutual inductance between the stator phases, the voltage applied across a phase equals the sum of the resistive voltage drop and the variation of the flux linkage [5–7]. This voltage is given by the following equation (1).

$$V = R_s i + \frac{\mathrm{d}\Phi}{\mathrm{d}t} = R_s i + \frac{\mathrm{d}L\left[L(\theta,i)i\right]}{\mathrm{d}t}. \qquad (1)$$

Knowing that θ is the rotor position, Φ the magnetic flux, eq. (1) can be written as

$$V = R_s i + L(\theta,i)\frac{\mathrm{d}i}{\mathrm{d}t} + \frac{\mathrm{d}L(\theta,i)}{\mathrm{d}t}\omega_m i. \qquad (2)$$

The three terms on the right side given by eq. (2) represent respectively the resistive voltage drop, the inductive voltage drop, and the induced electromotive force.

[1]Institute of maintenance and industrial security, Oran University 2. AB (ALGERIA) chouitek98@yahoo.com.
[2] REES Renewable Energies and Electrical Systems Laboratory. Faculty of Electrical Engineering Abdelhamid Ibn Badis Mostaganem University (ALGERIA). E-mails: ikchaouchdz@yahoo.fr, bekbenm@yahoo.fr

The following equation obtains the induced electromotive force e:

$$e = \frac{\mathrm{d}L(\theta,i)}{\mathrm{d}t}\omega_m = K_b\omega_m i\,, \tag{3}$$

$$\omega_m = \frac{\mathrm{d}\theta}{\mathrm{d}t}, \tag{4}$$

where ω_m is the rotational speed, e the expression of the electromotive force.

The multiplication by the instantaneous current on both sides given by equation (2) gives:

$$P_i = V \times i = R_s i^2 + \frac{\mathrm{d}L(\theta,i)}{\mathrm{d}t}\omega_m i^2 + L(\theta,i)i\frac{\mathrm{d}i}{\mathrm{d}t}, \tag{5}$$

where P_i is the instantaneous input power. The last term is not physically interpretable. It must be according to known variables to have a physical meaning.

$$\frac{\mathrm{d}}{\mathrm{d}t}\left(\frac{1}{2}L(\theta,i)i^2\right) = L(\theta,i)i\frac{\mathrm{d}i}{\mathrm{d}t} + \frac{1}{2}i^2\frac{\mathrm{d}L(\theta,i)}{\mathrm{d}t}. \tag{6}$$

Replacing in (5):

$$P_i = R_s i^2 + \frac{\mathrm{d}}{\mathrm{d}t}\left(\frac{1}{2}L(\theta,i)i^2\right) + \frac{1}{2}i^2\frac{\mathrm{d}L(\theta,i)}{\mathrm{d}t}. \tag{7}$$

This equation clearly shows that the instantaneous input power is equal to the sum of the resistive losses given by $R_s i^2$ the rate of change of the electromagnetic energy is given by $\frac{\mathrm{d}}{\mathrm{d}t}\left(\frac{1}{2}L(\theta,i^2)i^2\right)$ and the power P in the air gap given by the term $\frac{1}{2}i^2\frac{\mathrm{d}L(\theta,i)}{\mathrm{d}t}$.

Setting the time according to rotor position and speed

$$\frac{t}{\omega_m}. \tag{8}$$

The power P_a in the gap becomes

$$P_a = \frac{1}{2}i^2\frac{\mathrm{d}L(\theta,i)}{\mathrm{d}t} = \frac{1}{2}i^2\frac{\mathrm{d}L(\theta,i)}{\mathrm{d}t}\frac{\mathrm{d}\theta}{\mathrm{d}t} = \frac{1}{2}i^2\frac{\mathrm{d}L(\theta,i)}{\mathrm{d}t}\omega_m \tag{9}$$

He powers in the air gap is equal to the product of the electromagnetic torque T_e and the speed of the rotor ω_m

$$P_a = T_e\omega_m \tag{10}$$

By identification, we determine the equation of the electromagnetic torque knowing that the current i is constant

$$T_e = \frac{\mathrm{d}L(\theta,i)}{\mathrm{d}\theta} \times \frac{i^2}{2}, \tag{11}$$

$$\frac{\mathrm{d}L(\theta,i)}{\mathrm{d}\theta} = \frac{L(\theta_2,i) - L(\theta_1,i)}{\theta_2 - \theta_1}. \tag{12}$$

This variation of the inductance developed in eq. (12) will be considered the torque constant and expressed in N·m/A^2.

3. FEEDING THE VARIABLE RELUCTANCE MACHINE

The power supply by rectangular currents allows a gain in torque using a simple and robust power converter [8]. The asymmetric half-bridge inverter is used most for supplying the variable reluctance motor (see Fig 3).

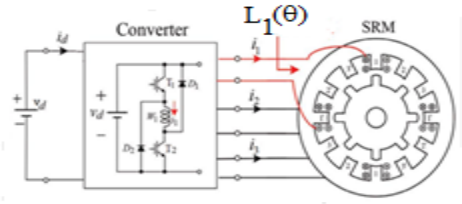

Fig. 3 – Supply of the SRM with an asymmetric half-bridge inverter.

An inverter arm is formed by two semiconductor switches and two free wheel diodes. The major advantage of this circuit is the independent phase control it.

4. CONTROL OF THE SRM WITH A CONVENTIONAL PID

The closed-loop control of the dc drive system is shown in Fig. 4. The power circuit consists of an asymmetric converter that drives the variable reluctance motor [9]. The circuit has an internal current control loop and an external loop for speed control. The variable speed drive is designed to follow the load variation. The current loop is used to generate the motor control signal V_d.

The performance of the PID controller for controlling the variable reluctance motor is simulated by varying the reference speed and the load. The parameters of the PID regulator are chosen optimally by known methods such as the imposition of poles, Ziegler, and Nichols.

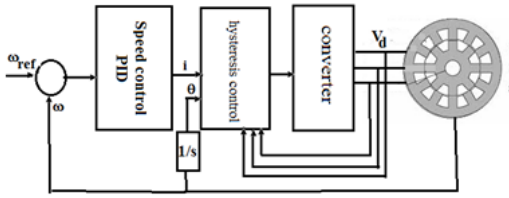

Fig. 4 –Controlling the SRM with a conventional PID controller

The best current, velocity, and torque responses were obtained by choosing the following values of the parameters of the PID regulator: K_p = 10, K_i = 8 and K_d = 0.5. These values were obtained after several tests.

5. THE PERFORMANCE OF THE PID CONTROLLER FOR CONTROLLING

Because of how the torque is produced in the form of pulses, the SRM is particularly susceptible to producing large torque ripples. These undulations are generally undesirable, especially in the field of traction, where oscillations of the motor can cause dangerous situations.

The conventional control algorithms, for example, with derivative integral proportional control, may prove sufficient if the requirements for the accuracy and performance of the systems are flexible. On the contrary case, and especially when the controlled part is subjected to solid no-linearity and temporal variations, intelligent

control techniques must be devised to ensure the process's robustness concerning the uncertainties on the parameters and their variations [10].

5.1. SRM NEURAL CONTROL

The principle of this control is based on inverse model identification. Figure 5 shows the inverse control scheme by neural networks.

The reference input ωr is compared with the output y of the process to form the tracking error $e = \omega - \omega_r$, which is used to modify the parameters of the network. After taking the inverse model, the neuro-controller delivers the output u of the RNC, which is the command injected at the process's input, the error is zero, and the output y is equal to the reference ω_r [11].

The simulation was performed with 10 hidden layers and an average final error of 0.00012 between the reference velocity and the output of the neuronal controller.

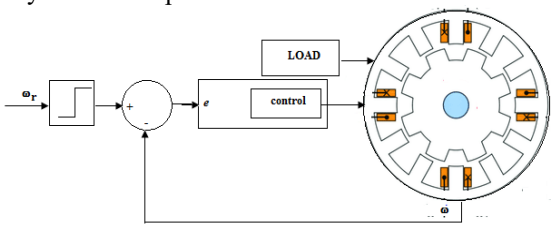

Fig. 5 – Neural network controller applied to SRM 12-8.

5.2. APPLYING THE FUZZY CONTROLLER TO THE SPEED SETTING

The objective is to design a fuzzy PID controller illustrated in Fig. 6 to maintain the speed of the variable reluctance motor at the desired set points, then introduce a stage where the motor is loaded and observe the controller's performance. It must at every moment to adapt different variations of speed [12].

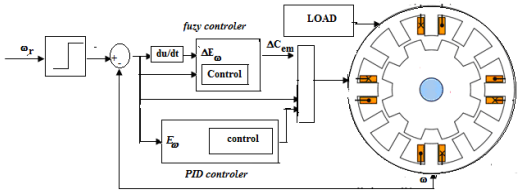

Fig. 6 – Block diagram of FUZZY-PID controller to SRM 12-8.

A PID – fuzzy controller replaces the conventional controller to ensure a 10% better operation by maintaining the set point speed even when charging the motor.

The conventional regulator PID is replaced by a fuzzy regulator of the type Sugeno whose linguistic variables are |20]:

- The inputs are the error, and the error variation is denoted respectively, E_ω and ΔE_ω .
- The output is ΔC_{em}.

In the case of speed control, the error [13] is usually used

$$E_\omega(k) = G_{E_\omega}\left(\omega_{ref}(k) - \omega(k)\right), \tag{13}$$

and the variation of the error ΔE_ω:

$$\Delta E_\omega(k) = G_{\Delta E_\omega}\left(E_\omega(k) - E_\omega(k-1)\right). \tag{14}$$

$G_{E\omega}$ and $G_{\Delta E\omega}$ represent the adaptation gains; they are chosen to be low for the system's stability. They play a crucial role. Indeed, these are the ones that will fix the performance of the command. This law is a function of error and its variation:

$$\Delta C_{em} = f\left(E_\omega, \Delta E_\omega\right) \tag{15}$$

5.2.1 STRUCTURE OF THE FUZZY CONTROL

We retained the controller:

- Input variables whose membership functions of the fuzzy sets are triangular and trapezoidal.
- E_ω and ΔE_ω are standardized in a discourse universe [-5, + 5], [-2.5, + 2.5]. See Fig. 7.
- The output variable ΔC_{em} is normalized in a speech universe [-40, + 40], see Fig. 8.

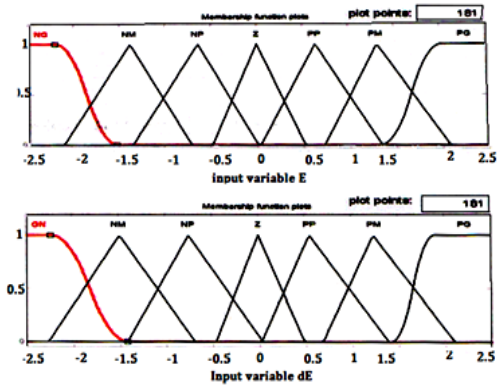

Fig. 7 –The membership functions for the input variables.

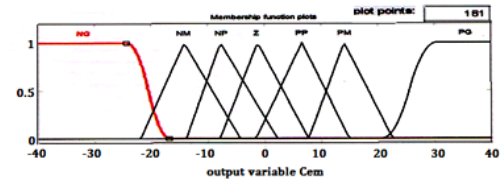

Fig. 8 –The membership functions for the output variable

An incremental PID structure (two-dimensional inference matrix). Based on the controller's operation and the machine's behavior, we deduce the rules of fuzzy inferences [14].

- Fuzzy rules, allowing determining the variable of the regulator's output according to the inputs' variables, are deduced from the table of Mac-Vicar called inference. In this case, it contains 49 rules, as shown in the inference table below in Table 2. The interval of each linguistic variable is subdivided into seven classes. To each of the classes, we associate a membership function. Based on the operation of the controller and the behavior of the machine, the following fuzzy inference rules are deduced:
- We try to reproduce intuitively to react when we are far from the objective, the fuzzy sets “big negative” and “big positive”, knowing that often, in this case, the actual output of the regulator will have reached its saturation limit value. When close to the reference speed, the “small negative” and "small positive" fuzzy sets will be solicited, and their membership functions will be closer to that of the “zero” set. The answer will be sweeter when one is far from the objective.
- Variable gains at the input and output of the regulator

to adjust its operation and vary its sensitivity range.

Table 2

Inference table with seven fuzzy sets

E_ω / ΔE_ω	BN	MN	SN	Z	SP	MP	BP
BN	BN	BN	BN	BN	MN	SN	Z
MN	BN	MN	SN	Z	SP	BN	BN
SN	MN	SN	Z	SP	MP	BN	MN
Z	SN	Z	SP	MP	BP	BN	SN
SP	Z	SP	MP	BP	BP	SN	Z
MP	BP	MP	BP	BP	BP	Z	SP
BP	BP	MP	BP	BP	BP	BN	BN

6. ORDER SIMULATION RESULTS

The simulation tool used is Mathwork MATLAB version 7.5. It is a mathematical calculation tool based on matrix calculation. It offers a library of specific functions for developing control algorithms under a Simulink graphical environment.

The block diagram of the simulation studies the dynamic behavior of the closed-loop SRM fed by the half-bridge inverter. It is a linear model representative of the three phases of our machine. The global converter-machine model and its control is obtained by associating the operation of the three offset angles of $\pi/6$.

The different phase currents of the stator winding, the torque developed in the motor, the speed of the latter are illustrated below

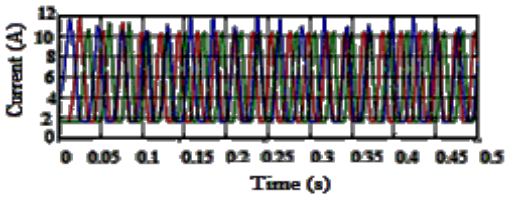

Fig. 9 –Total currents with PID controller.

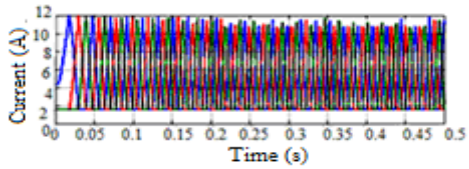

Fig. 10 – Total current with neuronal controller

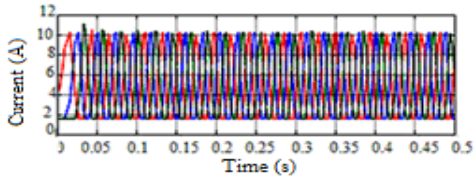

Fig 11 – Total current with a fuzzy controller

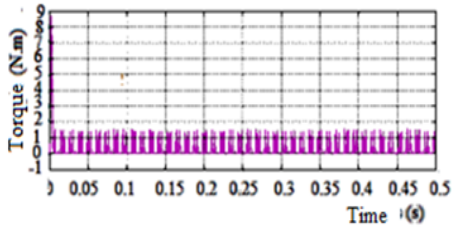

Fig 12 – Total torque with PID controller

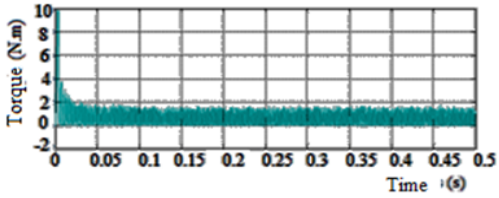

Fig. 13 – Total torque with neuronal controller.

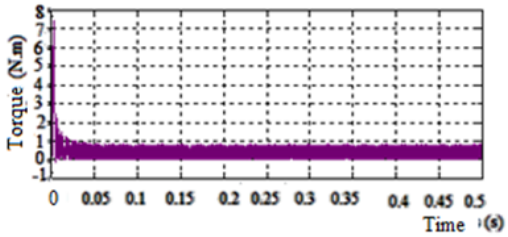

Fig. 14 – Total torque with a fuzzy controller.

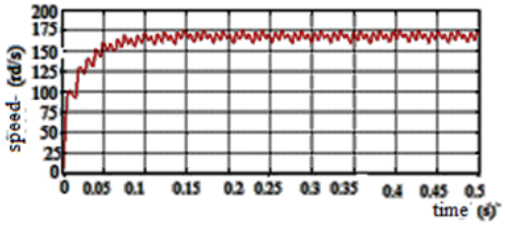

Fig. 15 – Speed with PID controller.

- The best results of the currents presented in Figs. 9-11 are obtained with the fuzzy controller. It is noted that the total current is stable, and the response time is fast. The overruns have disappeared entirely compared to the currents obtained with the neuronal or conventional PID controller.
- The total torque presented in Figs. 12-14 of the machine obtained by the PID controller is pulsating. It is less satisfactory when compared with the neuronal controller because the ripple band of the torque obtained by this controller is uniform and constant. Still, the fuzzy controller obtains the best result of Torque because this ripple band is minimal. It reaches 0.98 N·m.
- The speed response presented in Figs 15-16-17 obtained with the fuzzy controller is the best compared to the other neuronal or classical correctors because the undulations have faded and the overrun is almost zero, the reference is well followed since it reaches 200 rad/s.

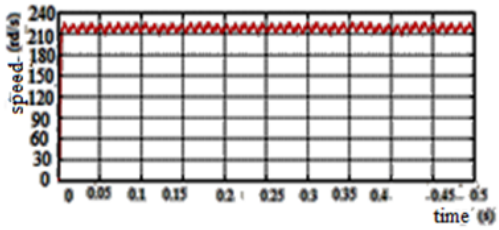

Fig. 16 – Speed with neuronal controller.

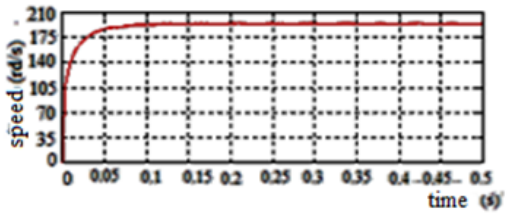

Fig. 17 – Speed with fuzzy controller.

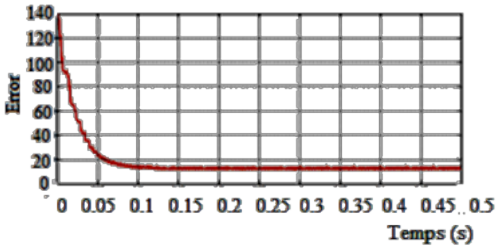

Fig. 18 – Speed error with neuronal controller.

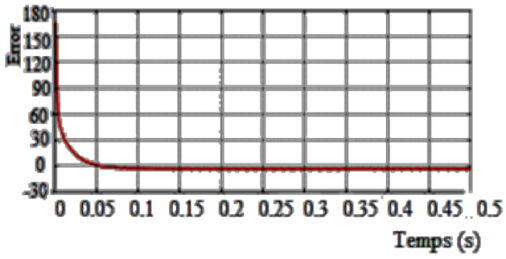

Fig. 19 – Error with the fuzzy controller.

It is noted that the error presented in Figs 18-19 is more important for a neuronal controller; it has decreased until canceled with the fuzzy controller.

The results obtained concerning the application of the fuzzy control show a marked improvement in the performance of the phase currents and the torque, but the best improvement is manifested in the quality of the velocity signal because the ripple bandwidth has been reduced to the maximum.

7. ROBUSTNESS STUDY OF CONTROLLERS USING ARTIFICIAL INTELLIGENCE

To test the neuronal control algorithm's or fuzzy control's robustness, parametric variations are imposed [14–17]. The variation in the inductance due to the derivative of this quantity or to a misidentification of this parameter directly affects the energy and the co-energy, which directly influence the speed of rotation and the torque of the switched Reluctance machine (SRM) see Figs. 20-23. By varying the maximum and minimum inductance values by +10 % (L_{max} = 90 mH and L_{min} = 60 mH).

It is observed that, despite the parametric variations, the behavioral changes of the adaptive fuzzy controller are not important, and the behavior in regulation and tracking remains very reliable. Indeed, disturbances are rejected very quickly. The adaptive blur controller is robust.

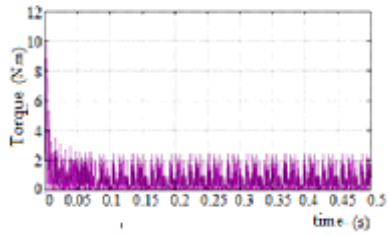

Fig. 20 – Total torque with neural controller with a 10% increase in inductance values L_{max} and L_{min}

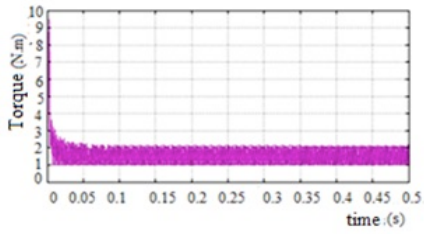

Fig 21 – Total torque with fuzzy controller with a 10 % increase in inductance values L_{max} and L_{min}

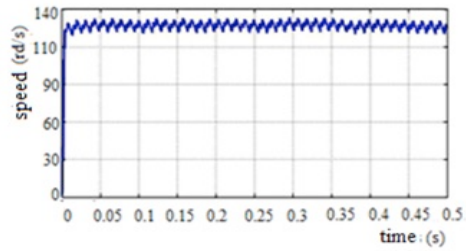

Fig. 22 – Speed with the neuronal controller with a 10 % increase in inductance values L_{max} and L_{min}.

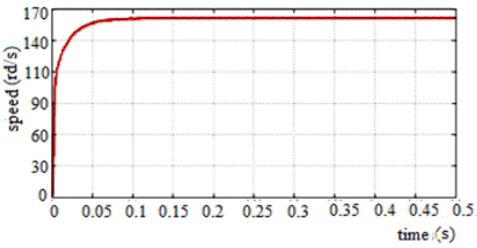

Fig. 23 – Speed with fuzzy controller with a 10 % increase in inductance values L_{max} and L_{min}.

8. CONCLUSION

The variable reluctance motor has a simple construction. Still, its mathematical model is difficult, due to its nonlinear behavior because its flux is a function of two variables: the current *i* and the position of the rotor θ.

The PID controller achieves good performance for one operating point, but it fails in the case of our 12/8 machine, which is highly nonlinear.

The torque of this machine is very pulsating, so it is only possible to obtain good dynamic performance with a simple linear control like the PID controller.

We presented two nonlinear control studies (neural and fuzzy) that compensate for motor nonlinearities and reduce torque ripples even in the presence of parametric uncertainties in the model.

The fuzzy logic controller is the best to improve the system's steady state accuracy, and when the error is large, this controller is used to speed up the dynamic response speed. The mad controller is also the most flexible, and its

response is relatively fast compared to the neural regulator's. It can be concluded that the fuzzy controller stabilizes the speed quite quickly, with a smooth response, and improves the dynamic behavior of the motor. This response is without overshoot, thus leading to better performance and high robustness.

Received on 19 March 2022

REFERENCES

1. O.K. Krinah, R. Lalalou, Z. Ahmida, S. Oudina, *Performance investigation of a wind power system based on double-feed induction generator: fuzzy versus proportional integral controllers*, Rev. Roum. Sci. Techn. – Électrotechn. Et Énerg., **67**, *4*, pp. 403–408, Bucarest (2022).
2. K.R. Chichate, S.R. Gore, A. Zadey, *Simulation of Switched Reluctance Motor for Speed Control Applications*, 2nd International Conference on Innovative Mechanisms for Industry Applications (ICIMIA), Bangalore, India (5-7 March 2020).
3. J.W. Ahn, G.F. Lukman, *Switched reluctance motor: Research trends and overview*, CES Transactions on Electrical Machines and Systems, **2**, *4*, pp. 339 - 347 (Dec. 2018).
4. D.F. Valencia, R. Tarvirdilu-Asl, C. Garcia, J. Rodriguez et al. *A review of predictive control techniques for switched reluctance machine drives*. Part I: Fundamentals and Current Control, IEEE Transactions on Energy Conversion, **36**, *2*, pp. 1313 - 1322 (29 Dec 2020).
5. A. Tahour, A.G. Aissaoui, A.C. Megherbi, *Position control of switched reluctance motor using an adaptive backstepping controller*, Rev. Roum. Sci. Techn. – Électrotechn. Et Énerg., **56**, *3*, pp. 314-324 (2011).
6. J. Han, G. Baojun, K. Zhang, Y. Wang, C. Wang, *Influence of control and structure parameters on the starting performance of a 12/8 pole switched reluctance*, Energies, A6: Electric Vehicles, **13**, *14*, pp. 3744, July (2020).
7. I.A. Viorel, L. Strete, I.F. Soran, *Analytical flux linkage model of switched reluctance motor*, Rev. Roum. Sci. Techn. – Électrotechn. Et Énerg.,**54**, *2*, pp. 139–146, Bucarest (2009).
8. P. Srinivas, *Implementation of PWM control of dc split converter fed switched reluctance motor drive*. International Journal of Electrical and Computer Engineering IJECE. **7**, *2*, pp. 604-609 (April 2017).
9. M. Chouitek, *Control of a variable reluctance motor by the use of artificial intelligence*. Doctoral thesis, Université des Sciences et de la Technologie d'Oran Mohamed Boudiaf (2016).
10. A. Tahour, *Neural controller for a switched reluctance machine*, Revue Roumaine des Sciences Techniques - Série Électrotechnique et Énergétique, **53**, *4*, pp. 473-482 (2008).
11. M. Habbab, A. Hazzab, P. Sicard, *real time implementation of fuzzy adaptive PI-sliding mode controller for induction*, International Journal of Electrical and Computer Engineering, **8**, *5*, pp. 2883-2893 (2018)
12. E. Daryabeigi, A.H. Zarchi, G.R.A. Markadeh, J. Soltani, R.A, F. Blaabjerg, *Online MTPA control approach for synchronous reluctance motor drives based on emotional controller*. IEEE Transactions on Power Electronics, **30**, pp. 2157-2166 (2015).
13. M. Ferrari, N. Bianchi, E. Fornasiero, *Analysis of rotor saturation in synchronous reluctance and pm-assisted reluctance motors*. IEEE Transactions on Industry Applications, **51**, pp. 169-177 (2015)
14. D. Flieller, N.K. Nguyen, P. Wira, G. Sturtzer, D.O. Abdeslam, J. Merckle *Self-learning solution for torque ripple reduction for nonsinusoidal permanent magnet motor drives based on artificial neural networks*, IEEE Transactions on Industrial Electronics, **61**, pp. 655-666 (2014).
15. D. Csaba, A. Binder, *Design of compact permanenet-magnet synchronous motors with concentrated windings*, Rev. Roum. Sci. Techn. – Électrotechn. Et Énerg., **52** *2*, pp. 182-198 (2007).
16. K. Makhloufi, S. Zegnoun, A. Omari, I.K. Bousserhane, *Commande neuro-floue-glissant adaptatif d'unemachine synchrone linéaire,* Rev. Roum. Sci. Techn. – Électrotechn. Et Énerg., **67**, *4*, pp. 425–431, Bucarest (2022).
17. M. Gamal, H. Hashem, *Speed control of switched reluctance motor based on fuzzy logic controller*, Proc. of the 14th Int.l Middle East Power Systems Conference (MEPCON'10), Cairo University, Egypt. Paper ID 166, Pp. 19-21 (2010).